Numerical Modeling of a Wind Turbine Blade Deflection Sensing System Using the Moving Frame FDTD Method

Franek, Ondrej

Published in:
Proceedings of the 2018 20th International Conference on Electromagnetics in Advanced Applications, ICEAA 2018

DOI (link to publication from Publisher):
10.1109/ICEAA.2018.8520426

Publication date:
2018

Document Version
Accepted author manuscript, peer reviewed version

Numerical Modeling of a Wind Turbine Blade Deflection Sensing System Using the Moving Frame FDTD Method

Ondřej Franek
Department of Electronic Systems, APMS Section
Aalborg University
Aalborg, Denmark
of@es.aau.dk

***Abstract*—Moving frame finite-difference time-domain (MF-FDTD) method is applied to numerical modeling of a wind turbine blade deflection sensing system that uses an ultrawideband (UWB) wireless link along the blade. The moving frame in MF-FDTD follows the propagation of only relatively small important part of the UWB pulse and therefore brings substantial savings in simulation time compared to the original FDTD method operating on the entire blade. In this paper, concrete formulas for determining the extent of the moving frame are given, taking into account the effects of the numerical dispersion of the FDTD method on the UWB pulse extent. In the numerical experiment, the actual speedup for a simulation of a 58.7m long wind turbine blade is shown to be approx. 11.5×, reducing the running time from 17 to 1.5 hours.**

***Index Terms*—Ultrawideband propagation, FDTD**

I. Introduction

A wireless system capable of measuring deflection of a wind turbine blade has recently been introduced [1], [2]. The deflection (bending) of the blade is determined from the time of arrival of short pulses launched by an antenna near the blade tip and received by an antenna close to the root. The system is based on an existing ultrawideband (UWB) technology in the range 3.1–4.8 GHz. It detects the pulse arrival by using a modified correlator that locks onto the rising edge of the received pulse.

Due to aerodynamic noise and protection from lightning strikes, the tip antenna is placed inside the blade tip. This poses a challenge for the wireless link as it has to operate on non-line-of-sight conditions. The electromagnetic waves radiated from the tip antenna must penetrate the fiberglass shell of the blade and then travel towards the root with very low elevation angle from the fiberglass-air boundary. The multipath components of the received signal may then become very strong and prevent reliable detection of the pulse time of arrival.

In order to predict the link budget and to determine the optimum location of the root antennas, we have modeled the wave propagation along the 58.7m long blade using the finite-difference time-domain (FDTD) method [3]. The computational domain consisted of more than 10 billion cubical mesh cells with cell size of 5 mm, including 50 cell thick perfectly matched layers (PML) necessary to suppress reflections from the outer boundaries under low elevation angles. Total simulation time on a parallel cluster was over 17 hours, after load balancing the parallel processes [4].

Since the wave traveling along the wind turbine is created by an UWB pulse, the portion of cells in the computational domain with non-negligible magnitude of the fields is small during the entire simulation and the active region is steadily moving along the blade from the tip towards the root. Moreover, as the correlator locks onto the rising edge only, the amount of cells whose fields are important for the result is quite limited. By exploiting these properties we could significantly reduce the simulation time and speed up the optimizations.

In this paper, we demonstrate the application of the moving frame FDTD method [5]–[9] to reduce the computation time of an UWB pulse traveling along a 58.7m long wind turbine blade. We present concrete formulas for determining the extent of the moving frame and the expected speedup, based on the geometrical constellation of the wireless link, parameters of the UWB pulse and material properties and their distribution along the propagation path. It is also shown that under the right circumstances it is even possible to remove the PML layers from the simulation frame without affecting the results, and thus reduce the computational burden even further. The findings and practical considerations presented here are applicable to efficient computation of other problems with similar arrangement.

II. Theoretical Background

The deflection sensing system uses the time of flight of the UWB pulse along the wireless link between a transmitting (TX) antenna near the blade tip and a receiving (RX) antenna near the blade root (see Fig. 1) to determine the extent of the blade deflection under operating conditions. The time of arrival is obtained by a maximum a-posteriori (MAP)

This work was supported by the Innovation Fund Denmark (Innovations-Fonden) project of Intelligent Rotor for Wind Energy Cost Reduction (project code 34-2013-2). The author also gratefully acknowledges the support from the Danish e-Infrastructure Cooperation (DeIC) for the Linux cluster Fyrkat at Aalborg University, Denmark.

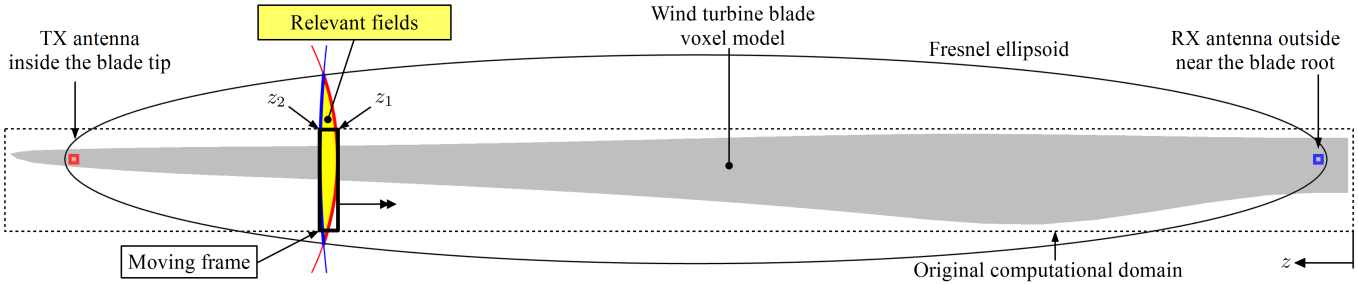

Fig. 1. Principle of the moving frame method: Only the fields in the yellow area are relevant at each particular time instant. The area is moving at constant speed from the tip (left) to the root (right) of the blade, as indicated by the double arrow. If the computational domain (dashed rectangle) is terminated by PML layers, only the fields inside the moving frame (bold rectangle) need to be evaluated.

correlation detector [10] that locks onto the rising edge of the incoming signal, so that any later arriving echos and multipath components are irrelevant. The useful pulse signal propagates between the TX and the RX antenna mostly along a straight line and in free space, except for a small portion of the propagation path at the blade tip, where the signal has to traverse the fiberglass shell on its way out of the blade. Here, due to refraction in the fiberglass shell (see Fig. 2), the signal travels with lower velocity and at a different angle than would correspond to a pure line-of-sight (LOS) conditions. However, this applies to a very small percentage of the wireless link, and the link is therefore assumed as being LOS in the following derivation of the method. The impact of the fiberglass shell and how to deal with it will be discussed later.

Fig. 1 depicts a two-dimensional cut through the space occupied by the wind turbine blade, and represents a situation at a certain time instant during the time of flight of the UWB pulse between TX and RX. The segment of the red circle centered at the TX antenna (denoted by a red square) represents a cut through the spherical pulse wavefront, which means that the space outside of this sphere has not yet been affected by the pulse. On the other hand, the segment of the blue circle centered at the RX antenna (blue square) represents the spherical boundary behind which no field will have a chance to affect the LOS pulse received at the RX antenna. As time progresses, the radius of the red sphere increases while the radius of the blue sphere decreases. It is only the intersection of the two spheres (denoted by yellow filling) where the electromagnetic fields need to be calculated by the FDTD method. Everything to the right of this volume has not been excited yet and has essentially zero field, while everything to the left will not reach the receiver in time to affect the LOS pulse. The idea of the moving frame method is to calculate the EM fields only in a small segment of the computational domain encompassing this volume instead of the entire domain occupied by the blade, and therefore reduce the running time accordingly.

The Gauss-sine pulse used in the simulation is shown in Fig. 3, with its total width denoted w_P. Its analytical representation is

$$f(t) = \mathrm{e}^{-\frac{1}{2}\left(\frac{t-t_0}{\tau_0}\right)^2} \mathrm{e}^{\mathrm{j}\omega_0(t-t_0)} \tag{1}$$

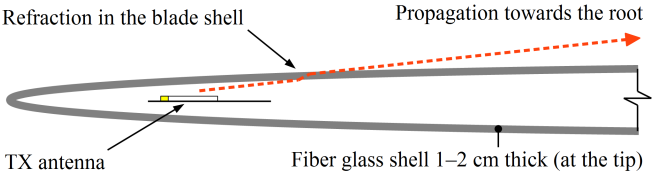

Fig. 2. Detail of the blade tip with the TX antenna inside. The pulse propagation path (red dashed line) traverses the blade shell (grey) with refraction.

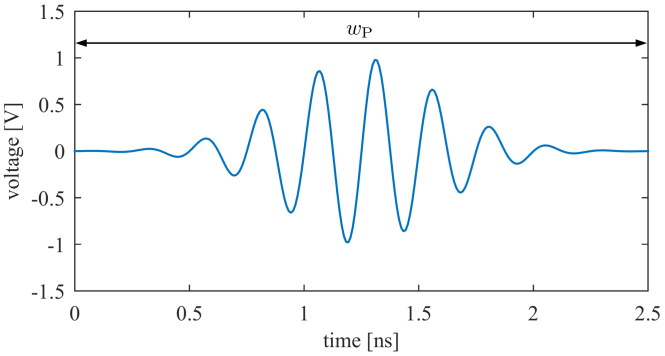

Fig. 3. The Gauss-sine pulse used in the simulations.

where $\omega_0 = 2\pi f_0$ with f_0 being the center frequency, t_0 is the time offset of the envelope peak, and τ_0 is the effective width of the pulse envelope.

Under normal conditions, the pulse would propagate in free space with speed of light c and its width would stay the same. However, the FDTD method suffers from numerical dispersion [3], hence the pulse will propagate with speed smaller than c and the envelope will be spread in time and space. This needs to be taken into account when calculating the extent of the moving frame.

The numerical dispersion relation of the Yee staggered leap-frog FDTD with wavevector $\tilde{k} = (\tilde{k}_x, \tilde{k}_y, \tilde{k}_z)$ is [3], [11]

$$\left[\frac{1}{c\Delta t}\sin\frac{\omega\Delta t}{2}\right]^2 = \sum_{\xi\in x,y,z}\left[\frac{1}{\Delta\xi}\sin\frac{\tilde{k}_\xi\Delta\xi}{2}\right]^2 \tag{2}$$

where $\Delta x, \Delta y, \Delta z$ are the cell dimensions of the FDTD grid, Δt is the time step, and f in $\omega = 2\pi f$ is the frequency. In our

case, the propagation takes place mostly in the direction along the blade, or very closely to it, which is a direction that is also parallel to the discretization grid. We can therefore assume that the dispersive wavenumber $\tilde{k}$ is the one corresponding to the z coordinate direction, namely

$$\tilde{k} = \tilde{k}_z = \frac{2}{\Delta z} \arcsin\left(S^{-1} \sin \frac{\omega \Delta t}{2} \right) \tag{3}$$

where $S = c\Delta t/\Delta z$ is the Courant factor which should be set close to $1/\sqrt{3}$ in order to get minimum dispersion error.

From (3) we determine the first and the second derivatives of the wavenumber at the pulse center frequency f_0

$$\tilde{k}_0' = \left. \frac{\mathrm{d}\tilde{k}}{\mathrm{d}\omega} \right|_{\omega = 2\pi f_0} \qquad \tilde{k}_0'' = \left. \frac{\mathrm{d}^2\tilde{k}}{\mathrm{d}\omega^2} \right|_{\omega = 2\pi f_0} \tag{4}$$

The group velocity v_g with which the pulse propagates through the dispersive grid is the reciprocal of the first derivative of $\tilde{k}$,

$$v_\mathrm{g} = (\tilde{k}_0')^{-1} \tag{5}$$

If the pulse propagates on distance R (the largest distance between the TX and RX), then the moving frame width reaches

$$w_\mathrm{MF} = v_\mathrm{g} w_\mathrm{P} \frac{\tau}{\tau_0} \tag{6}$$

where τ is the effective width of the pulse envelope after traveling distance R in dispersive media [12]

$$\tau = \sqrt{\tau_0^2 + \left(\frac{\tilde{k}_0'' R}{\tau_0} \right)^2} \tag{7}$$

The lower and upper limits of the moving frame along the z coordinate, z_1 and z_2, respectively, can be approximately calculated as

$$z_1 = z_\mathrm{TX} - v_\mathrm{g} t \tag{8}$$

$$z_2 = z_1 + w_\mathrm{MF} \tag{9}$$

where z_TX is the z-axis coordinate of the TX antenna and t is the time from the simulation start (assuming the pulse is launched immediately after start). Regarding the signs in (8) and (9), it should be noted that the z coordinates are increasing in the direction from the root to the tip of the blade, whereas the direction of propagation is opposite, ie. from the tip to the root.

In the derivation above, the extent of the moving frame has been determined assuming free space propagation only. This assumption is valid for the most of the propagation path except a small portion at the tip, where the pulse has to traverse the 1–2 cm thick fiberglass shell of the blade (see Fig. 2). It can therefore be expected that the pulse will be slightly delayed and more dispersed compared to pure LOS conditions. Consequently, the extent of the moving frame should be adjusted to accommodate the slower and longer pulse. This would usually be done by modifying the speed of light c in (2) to correspond to the media which the pulse propagates through. Alternatively, if the portion of the propagation path in media other than air is very small, as in our case, the limits of the moving frame (8) and (9) could simply be extended by small margins in each direction. As will be shown in the next section, this measure was not necessary in our case, as the received pulse in the moving frame is in very good agreement with the reference pulse, even using the original limits (8) and (9).

So far, only the longitudinal, ie. z, coordinates of the moving frame have been discussed. The transverse extent of the frame is generally governed by the size of the Fresnel ellipsoid (depicted in Fig. 1), which depends on the pulse width w_P or any other time frame of the received pulse we may be interested in. In our case, the cross section of the Fresnel ellipsoid is larger than the extent of the blade voxel model, so the moving frame will encompass the entire cross section of the original computational domain, which is terminated by the PML layers emulating free space in the transversal directions. If, however, the cross section of the Fresnel ellipsoid was smaller than the original computational domain, then the transversal extent of the moving frame could also be smaller. Most importantly, the PML layers at the outer boundaries of the domain could then be entirely omitted. This can be a large benefit because the PML for grazing incidences that occur on elongated computational domains must be very thick to be effective, e.g. 50 cells in our case.

The theoretical expected speedup of the method can be calculated as the ratio of the number of cells in the moving frame to the total number of cells in the computational domain along z dimension, provided that the mesh cell size Δz is constant. If the mesh cell size is variable, the number of cells in the moving frame must be averaged over all time steps

$$\mathrm{Speedup} = \frac{1}{m_\mathrm{max} n_\mathrm{max}} \sum_{m_\mathrm{max}} (n_2 - n_1) \tag{10}$$

where m_max is the total number of time steps, n_max is the total number of mesh cells along z dimension, and n_1 and n_2 are the integer coordinates of the cells corresponding to the moving frame boundaries z_1 and z_2 as presented in (8) and (9), respectively. However, the true speedup is always smaller due to overhead in the FDTD code, as can be seen from the numerical experiment described in the next section.

III. Numerical Experiment

The moving frame technique has been used to speed up the computation of the signals at the blade root performed with our in-house FDTD code. The receiving point was at $z_\mathrm{RX} = 2$ m from the blade root whereas the TX antenna was placed inside the blade near the tip at $z_\mathrm{TX} = 56.45$ m. Total length of the blade was 58.7 m and it was included as a voxel model with cubical voxels of the same size as the cells in the FDTD grid, $\Delta x = \Delta y = \Delta z = 5$ mm. The Gauss-sine pulse (1) covered frequency band 3–5 GHz with central frequency $f_0 = 4$ GHz, envelope peak offset $t_0 = 1.25$ ns, total width $w_\mathrm{P} = 2t_0 = 2.50$ ns, and effective width $\tau_0 = 9.62$ ps.

Fig. 4 shows the co-polarized electric field at the position of the root RX antenna for both full domain and moving frame simulations. It can be seen that the moving frame technique recreates the received pulse almost exactly. The displayed

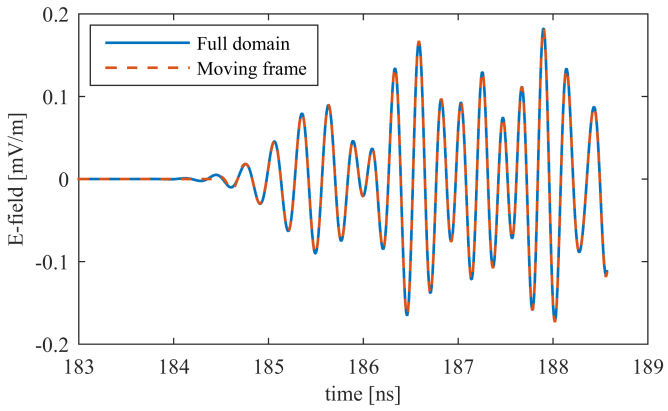

Fig. 4. Comparison of the E-fields at the RX point with the wind turbine blade voxel model from full-domain FDTD simulation (blue) and from simulation using the moving frame FDTD technique (red dashed).

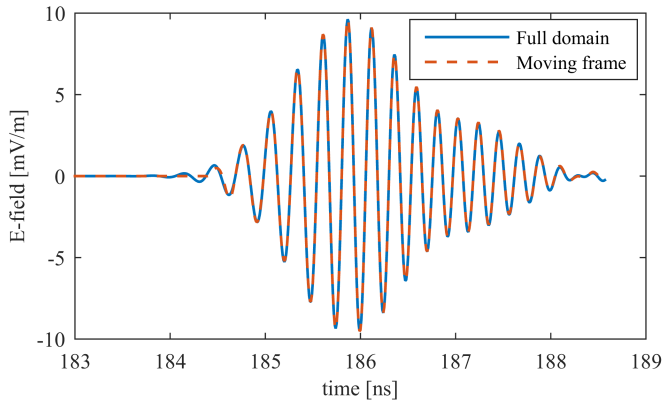

Fig. 5. Comparison of the E-fields at the RX point in empty space (no blade model present) from full-domain FDTD simulation (blue) and from simulation using the moving frame FDTD technique (red dashed).

pulse has not been treated with dispersion compensation as in [8], [11], but it still shows that the pulse arrives distorted from multipath components due to the presence of the blade.

For comparison, the same simulation has been run without the blade voxel model, so the pulse propagates in free space without multipath distortion. The results are shown in Fig. 5 and again the match between the full domain and moving frame techniques is excellent, save for minor differences at the very start of the pulse. The observed distortion of the pulse is not due to the blade, but purely due to the numerical dispersion of FDTD.

Since the computational domain is 11925 cells long and the frame width was in this case constant with 330 cells, the expected speedup of the method would be 36×. However, due to overhead and parallel process configuration the actual speedup was close to 11.5×. This is still a significant improvement which allowed us to increase the turnover of optimization runs significantly, reducing the simulation time from 61750 s (over 17 hours) for the full domain FDTD to 5365 s (approx. 1.5 hours) with the moving frame technique.

IV. Conclusion

The moving frame FDTD method has been demostrated to be capable of successful modeling of UWB pulse propagation along a wind turbine blade. Compared to the "classic", full-domain FDTD, the simulation time has been reduced 11.5×, yet the fields at the reception points are in excellent agreement with those obtained by the FDTD method updating the entire computational domain. The position and the extent of the moving frame are expressed explicitly assuming free space propagation and taking into account the numerical dispersion of the FDTD method. It has been observed that the free-space assumption is sufficient and has no influence on the results, even though the UWB pulse has to penetrate the fiberglass blade shell and then propagate close to the blade surface. The implementation of the technique using the presented parameters is straightforward and should be easily applicable to other problems with similar arrangement.

Acknowledgment

The author would like to thank Peter Baek and Claus Byskov at LM Wind Power for providing the voxel model of the wind turbine blade used in the numerical experiment.

References

[1] S. Zhang, T. L. Jensen, O. Franek, P. C. Eggers, K. Olesen, C. Byskov, and G. F. Pedersen, "UWB wind turbine blade deflection sensing for wind energy cost reduction," *Sensors*, vol. 15, no. 8, pp. 19 768–19 782, 2015.

[2] S. Zhang, T. L. Jensen, O. Franek, P. C. Eggers, C. Byskov, and G. F. Pedersen, "Investigation of a UWB wind turbine blade deflection sensing system with a tip antenna inside a blade," *IEEE Sensors Journal*, vol. 16, no. 22, pp. 7892–7902, 2016.

[3] A. Taflove and S. C. Hagness, *Computational electrodynamics: The Finite-Difference Time-Domain Method*, 3rd ed. Boston: Artech house, 2005.

[4] O. Franek, "A simple method for static load balancing of parallel FDTD codes," in *2016 International Conference on Electromagnetics in Advanced Applications (ICEAA)*. IEEE, 2016, pp. 587–590.

[5] F. Akleman and L. Sevgi, "A novel finite-difference time-domain wave propagator," *IEEE Transactions on Antennas and Propagation*, vol. 48, no. 5, pp. 839–841, 2000.

[6] R. Luebbers, J. Schuster, and K. Wu, "Full wave propagation model based on moving window FDTD," in *Military Communications Conference, 2003. MILCOM'03. 2003 IEEE*, vol. 2. IEEE, 2003, pp. 1397–1401.

[7] J.-P. Bérenger, "FDTD computation of VLF-LF propagation in the Earth-ionosphere waveguide," in *Annales des Télécommunications*, vol. 57, no. 11-12. Springer, 2002, pp. 1059–1090.

[8] ——, "Long range propagation of lightning pulses using the FDTD method," *IEEE transactions on electromagnetic compatibility*, vol. 47, no. 4, pp. 1008–1011, 2005.

[9] T. Oikawa, J. Sonoda, M. Sato, N. Honma, and Y. Ikegawa, "Analysis of lightning electromagnetic field on large-scale terrain model using three-dimensional MW-FDTD parallel computation," *Electrical Engineering in Japan*, vol. 184, no. 2, pp. 20–27, 2013.

[10] T. L. Jensen, M. L. Jakobsen, J. Østergaard, J. K. Nielsen, C. Byskov, P. Bæk, and S. H. Jensen, "Online estimation of wind turbine blade deflection with UWB signals," in *Signal Processing Conference (EUSIPCO), 2015 23rd European*. IEEE, 2015, pp. 1182–1186.

[11] O. Franek, S. Zhang, K. Olesen, P. C. F. Eggers, C. Byskov, and G. F. Pedersen, "Application of numerical dispersion compensation of the Yee-FDTD algorithm on elongated domains," in *2017 International Conference on Electromagnetics in Advanced Applications (ICEAA)*. IEEE, 2017, pp. 1243–1246.

[12] S. J. Orfanidis, *Electromagnetic waves and antennas*. Rutgers University New Brunswick, NJ, 2002.